AD-A047 404 NAVAL RESEARCH LAB WASHINGTON D C F/G 20/14
A METHOD-OF-MOMENTS SOLUTION FOR DISPERSION CHARACTERISTICS OF --ETC(U)
AUG 77 A K GANGULY, B E SPIELMAN
UNCLASSIFIED NRL-MR-3581 SBIE-AD-E000039 NL

1 OF 1
ADA047404

END
DATE FILMED
1-78
DDC

NRL Memorandum Report 3581

(12) 63

A Method-of-Moments Solution for Dispersion Characteristics of Arbitrarily-Configured Transmission Media

A. K. GANGULY and B. E. SPIELMAN

Microwave Techniques Branch
Electronics Technology Division

August 1977

NAVAL RESEARCH LABORATORY
Washington, D.C.

SECURITY CLASSIFICATION OF THIS PAGE (When Data Entered)

REPORT DOCUMENTATION PAGE

READ INSTRUCTIONS BEFORE COMPLETING FORM

1. REPORT NUMBER: NRL Memorandum Report 3581
2. GOVT ACCESSION NO.
3. RECIPIENT'S CATALOG NUMBER

4. TITLE (and Subtitle): A METHOD-OF-MOMENTS SOLUTION FOR DISPERSION CHARACTERISTICS OF ARBITRARILY-CONFIGURED TRANSMISSION MEDIA
5. TYPE OF REPORT & PERIOD COVERED: Interim report on a continuing NRL problem.
6. PERFORMING ORG. REPORT NUMBER

7. AUTHOR(s): A.K. Ganguly and B.E. Spielman
8. CONTRACT OR GRANT NUMBER(s): 61153N, 62762N

9. PERFORMING ORGANIZATION NAME AND ADDRESS: Naval Research Laboratory, Washington, D.C. 20375
10. PROGRAM ELEMENT, PROJECT, TASK AREA & WORK UNIT NUMBERS: NRL Problems R08-63 & R08-43G; Projects RR021-03-46 & XF54 581-004

11. CONTROLLING OFFICE NAME AND ADDRESS
12. REPORT DATE: August 1977
13. NUMBER OF PAGES: 34

14. MONITORING AGENCY NAME & ADDRESS (if different from Controlling Office): 34p.
15. SECURITY CLASS. (of this report): UNCLASSIFIED
15a. DECLASSIFICATION/DOWNGRADING SCHEDULE

16. DISTRIBUTION STATEMENT (of this Report): Approved for public release; distribution unlimited. NRL-MR-3581

RR021-03, RR021-03-46, XF54581004, F54581

17. DISTRIBUTION STATEMENT (of the abstract entered in Block 20, if different from Report)

SBIE, AD-E000 039

18. SUPPLEMENTARY NOTES

19. KEY WORDS (Continue on reverse side if necessary and identify by block number)

Computer-aided analysis
Transmission lines
Dispersion
Higher-order modes
Microwave integrated circuits
Millimeter-wave integrated circuits
Method of moments

20. ABSTRACT (Continue on reverse side if necessary and identify by block number)

A method for calculating the propagation characteristics of electromagnetic waves along arbitrarily configured transmission media composed of conductors and/or inhomogeneous dielectrics is presented. The method is based on the equivalence principle. The dispersion characteristics of the fundamental as well as higher order modes can be obtained by this method. To demonstrate the validity of this method, results of the propagation constant of a shielded microstrip line calculated by this method are compared with other numerical results available in the literature. New results for the dispersion characteristics of a channelized suspended microstrip are presented.

DD FORM 1 JAN 73 1473 EDITION OF 1 NOV 65 IS OBSOLETE
S/N 0102-014-6601

SECURITY CLASSIFICATION OF THIS PAGE (When Data Entered)

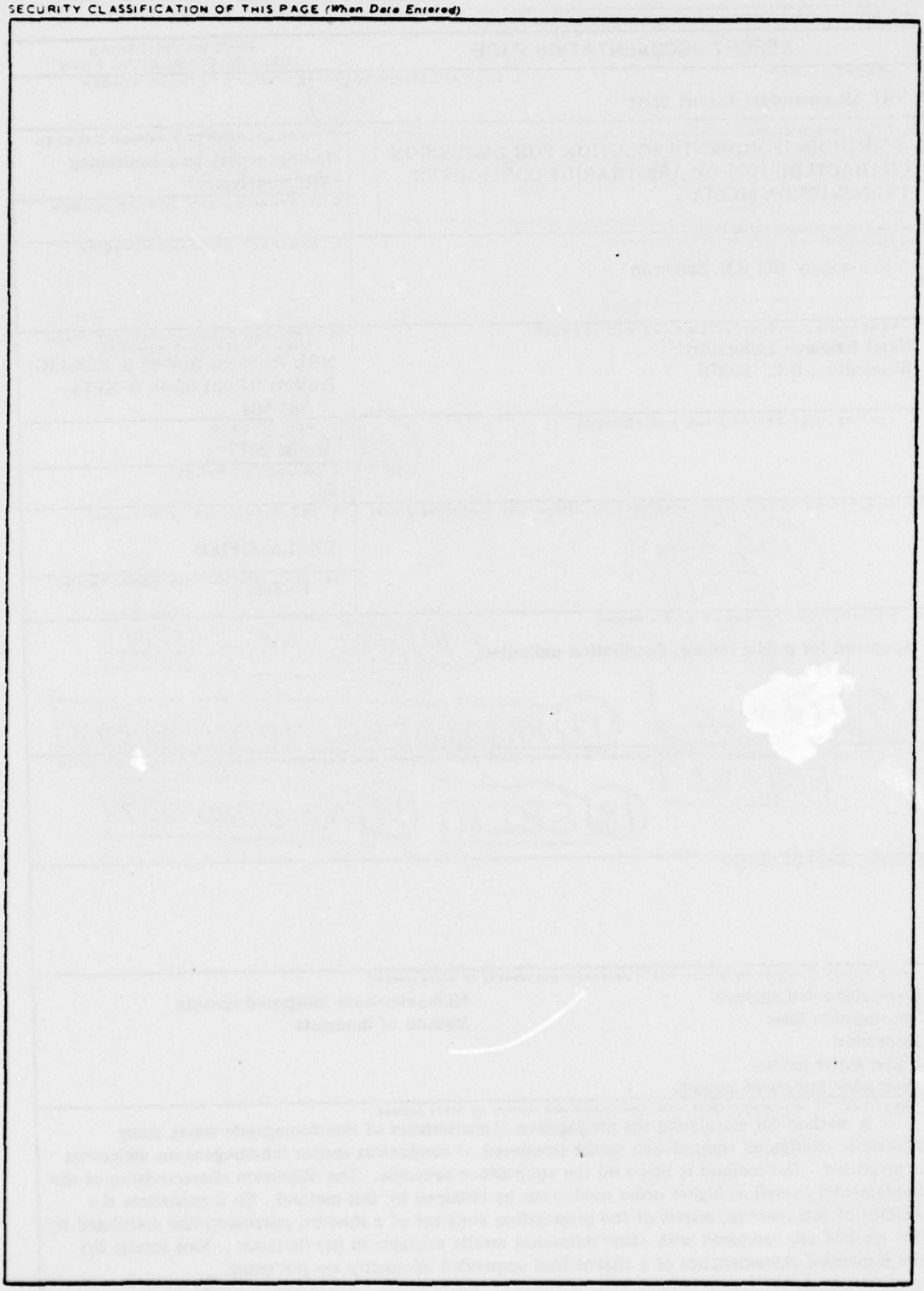

CONTENTS

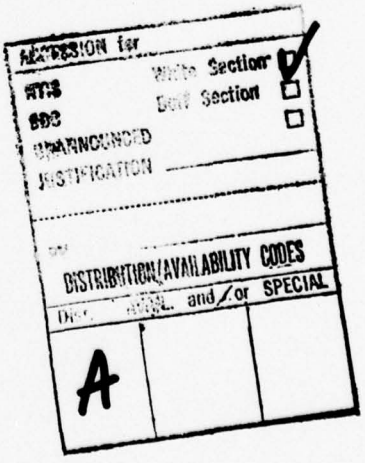

A METHOD-OF-MOMENTS SOLUTION FOR DISPERSION CHARACTERISTICS OF ARBITRARILY-CONFIGURED TRANSMISSION MEDIA

I. INTRODUCTION

The success of microstrip in microwave integrated circuit applications has caused considerable interest in the calculation of dispersion characteristics of these lines. A number of different techniques [1-4] have been employed to obtain dispersive effects of open and shielded microstrip-like transmission lines with rectangular cross-sections. Since microstrip becomes lossy and difficult to fabricate at higher microwave frequencies, attention has focused on configuring new transmission media. In this report we present a technique for calculating the dispersion characteristics of electromagnetic wave propagation along guiding structures consisting of a finite number of uniform dielectric regions of arbitrary cross-sections within a conducting enclosure. Conducting strips may also be present at the interface between two dielectric regions. It is assumed that the thickness of the conductors is negligible.

In Section II the problem is formulated on the basis of the equivalence principle. A set of linear integro-differential operator equations for the equivalent current sources are obtained by applying the appropriate boundary conditions at each interface. In Section III the operator equations are converted into a matrix formulation by the method

Note: Manuscript submitted July 29, 1977.

of moments [6,7,8]. The numerical methods used to determine the propagation characteristics and results for specific examples are described in Section IV.

II. INTEGRO-DIFFERENTIAL EQUATIONS

Fig.1 shows the generic cross-section of the guiding structure under consideration. N is the number of discrete homogeneous, isotropic dielectric regions inside the conducting enclosure. The heavy lines on the interface between two dielectric regions denote conducting strips. The electric $(\vec{E})$ and magnetic $(\vec{H})$ fields in each region will be obtained by applying the principle of equivalence [5]. In accordance with this principle the dielectric medium of the p-th region (characterized by permittivity ϵ_p) is fictitiously extended to fill all space and combinations of electric $(\vec{J}^p)$ and magnetic $(\vec{M}^p)$ surface current sources are conceptually placed on the boundary S_p of the p-th region. $\vec{J}^p$ and $\vec{M}^p$ are to be determined in such a way that $\vec{E}$ and $\vec{H}$ are zero everywhere outside S_p and are identical to the fields $\vec{E}^p$ and $\vec{H}^p$ at each point in the interior of the p-th region for the original problem shown in Fig. 1. This procedure is repeated for each of the regions inside the conducting enclosure. The current sources for the various regions are not all independent because of the boundary

conditions to be satisfied at all the interfaces. Fig.2 symbolically shows the contour of the p-th region and the surface current distributions on it. $\vec{M}^p$ is taken to be zero on the conducting segments of the boundary. Also shown in Fig.2 is a left-handed coordinate system with unit vectors $\hat{\tau}_p$, $\hat{n}_p$ and $\hat{z}$. $\hat{\tau}_p$ is tangential to the contour c_p (counterclockwise), $\hat{n}_p$ inward drawn normal to the region p and $\hat{z}$ perpendicular to the plane of Fig.2. For two adjacent regions p and p', we have $\hat{\tau}_p = -\hat{\tau}_{p'}$, and $\hat{n}_p = -\hat{n}_{p'}$, on the portion of boundary common to both the contours c_p and $c_{p'}$. $\hat{z}$ is the same for all regions. Since $\vec{J}^p$ and $\vec{M}^p$ are surface currents, we have the relations:

$$\begin{aligned} \hat{n}_p \cdot \vec{M}^p &= 0, \\ \hat{n}_p \cdot \vec{J}^p &= 0 . \end{aligned} \tag{1}$$

From the equivalence principle:

$$\begin{aligned} \vec{J}^p(\vec{\rho}, z) &= \hat{n} \times \vec{H}^{p-}(\vec{\rho}, z) \\ \vec{M}^p(\vec{\rho}, z) &= -\hat{n} \times \vec{E}^{p-}(\vec{\rho}, z) \end{aligned} \tag{2}$$

where $\vec{E}^{p-}$ and $\vec{H}^{p-}$ denote, respectively, the electric and magnetic fields at a point just inside the contour c_p. $\vec{\rho}$ is a position vector in the tangential plane. In equation (2) $\vec{\rho}$ is on c_p.

From Maxwell's equations the electric ($\vec{E}^p$) and magnetic ($\vec{H}^p$) fields at any point in the crosssection of Fig.2 may be written as

$$-\epsilon_p \vec{E}^p = \nabla \times \vec{F}^p + j \epsilon_p \omega \vec{A}^p + \epsilon_p \nabla \varphi_e^p \quad , \tag{3}$$

$$-\mu_o \vec{H}^p = -\nabla \times \vec{A}^p + j \mu_o \omega \vec{F}^p + \mu_o \nabla \varphi_m^p \quad , \tag{4}$$

where $p = 1, 2, \ldots, N$. $\vec{A}^p$ and φ_e^p are the vector and scalar potentials, respectively, due to the electric current sources ($\vec{J}^p$) residing on the contour c_p. Similarly, $\vec{F}^p$ and φ_m^p are the vector and scalar potentials, respectively, due to the magnetic current sources ($\vec{M}^p$) residing along c_p. μ_o is the free space permeability. In equations (3)-(4) a time dependence of $e^{i\omega t}$ has been assumed for the sources.

The potentials A, F, φ_e and φ_m are given by

$$\vec{A}^p(\vec{\rho}, z, t) = \mu_o e^{+i\omega t} \oint_{c_p} \vec{J}^p(\vec{\rho}', z) G(k_\rho^p R) d\tau' \quad , \tag{5}$$

$$\vec{F}(\vec{\rho}, z, t) = \epsilon_p e^{+i\omega t} \oint_{c_p} \vec{M}^p(\vec{\rho}', z) G(k_\rho^p R) d\tau' \tag{6}$$

$$\varphi_e^p(\vec{\rho}, z, t) = -(1/j\omega\epsilon_p)\, e^{i\omega t} \oint_{c_p} \nabla' \cdot \vec{J}^p(\vec{\rho}', z, t) G(k_\rho^p R) d\tau' \quad , \tag{7}$$

$$\omega_m^p(\vec{\rho}, z, t) = -(1/j\omega\mu_o)e^{i\omega t} \oint_{c_p} \nabla' \cdot \vec{M}^p(\vec{\rho}', z, t) G(k_\rho^p R) d\tau' \quad . \tag{8}$$

where $R = |\vec{\rho} - \vec{\rho}'|$ is the distance between a field point $(\vec{\rho})$ and a source point $(\vec{\rho}')$, $k_\rho^p = |\mu_o \epsilon_p \omega^2 + k_z^2|^{\frac{1}{2}}$ and $G(k_\rho^p R)$ is the two-dimensional Green's function. If $(\mu_o \epsilon_p \omega^2 + k_z^2)$ is positive, $G(x)$ can be expressed in terms of $H_o^{(2)}(x)$, the zero order Hankel function of the second kind, as

$$G(x) = (1/4j) H_0^{(2)}(x); \tag{9}$$

while for $(\mu\epsilon_p\omega^2 + k_z^2)$ negative

$$G(x) = (1/2\pi) K_0(x) \quad , \tag{10}$$

where $K_0(x)$ is the zero order modified Bessel function.

The gradient operators ∇ and ∇' operate on the field points and the source points respectively. The operator ∇' may be written as

$$\nabla' = \nabla_t' + \hat{z} \frac{\partial}{\partial z} \tag{11}$$

where ∇_t' is the tangential part of the vector. The electric $(\vec{E}^p)$ and magnetic $(\vec{H}^p)$ fields in the p-th can be calculated by substituting Eqs. Eqs. (5)--(10) in Eqs. (3) and (4). We assume that the sources vary as $e^{-k_z z}$ along the z-axis. For lossless propagation $k_z = i\beta$. By using the one-dimensional divergence theorem terms like $(\nabla_t' \cdot \vec{J}^p)G$ in Eqs.(7) and (8) may be expressed in the form $\vec{J}^p \cdot \nabla_t' G$. Furthermore, we have

$$\nabla_t' G(k_\rho^p R) = -\nabla_t G(k_\rho^p R) = -\hat{R}\, k_\rho^p \frac{\partial G(x)}{\partial x} \tag{12}$$

where $x = k_\rho^p R$ and $\hat{R} = (\vec{\rho} - \vec{\rho}')/R$ is the unit vector from the source point $(\vec{\rho}')$ to the field point $(\vec{\rho})$. Using these relations and after some vector manipulations the tangential components of $\vec{E}^p$ and $\vec{H}^p$ at a point P_- just inside the contour c_p may be expressed in the following form:

$$E_z^{p-} = j\mu_o\omega \left[-\int d\tau'\, J_{z'}^p\, G(x) \left\{ 1 + \frac{k_z^2}{\bar{\epsilon}_p k_o^2} \right\} + \frac{k_z\, k_\rho^p}{\bar{\epsilon}_p\, k_o^2} \int d\tau'\, J_{\tau'}^p\, \hat{\tau}' \cdot \hat{R}\, G'(x) \right.$$
$$\left. + \frac{k_\rho^p}{k_o} \int d\tau'\, \hat{n}' \cdot \hat{R}\, G'(x)\, \tilde{M}_{\tau'}^p \right] , \tag{13}$$

$$E_\tau^{p-} = j\mu_o\omega \left[\int d\tau'\, \frac{k_z k_\rho^p}{\bar{\epsilon}_p k_o^2}\, \hat{\tau} \cdot \hat{R}\, G'(x)\, J_{z'}^p \right.$$
$$- \int d\tau' J_{\tau'}^p \left\{ (\hat{\tau}' \cdot \hat{\tau}) \left(G(x) + \frac{k_\rho^p}{\bar{\epsilon}_p k_o^2 R} G'(x) \right) + \frac{(k_\rho^p)^2}{\bar{\epsilon}_p k_o^2} (\hat{\tau}' \cdot \hat{R})(\hat{\tau} \cdot \hat{R}) \cdot \right. \tag{14}$$
$$\left. \left(G''(x) - \frac{1}{k_\rho^p R} G'(x) \right) \right\}$$
$$\left. - \frac{k_\rho^p}{k_o} \int d\tau'\, G'(x)(n \cdot R)\, \tilde{M}_{z'}^p + \frac{k_z}{k_o} \int d\tau' (\hat{n}' \cdot \tau)\, G(x)\, \tilde{M}_{\tau'}^p \right] ,$$

$$H_z^p = (\mu_o \varepsilon_o)^{\frac{1}{2}} \omega \left[-\frac{k_\rho^p}{k_o} \int d\tau' \, J_\tau^p, \, \hat{n}' \cdot \hat{R} \, G'(x) + \bar{\varepsilon}_p \left(1 + \frac{k_z^2}{\bar{\varepsilon}_p k_o^2} \right) \int d\tau' \, \breve{M}_z^p, \, G(x) \right.$$

$$\left. - \frac{k_z k_\rho^p}{k_o^2} \int d\tau' \, \breve{M}_\tau^p, \, \hat{\tau}' \cdot \hat{R} \, G'(x) \right] , \tag{15}$$

$$H_\tau^p = (\mu_o \varepsilon_o)^{\frac{1}{2}} \omega \left[\frac{k_\rho^p}{k_o} \int d\tau' \, J_z^p, \, (\hat{n} \cdot R) \, G'(x) - \frac{k_z}{k_o} \int d\tau' \, J_\tau^p, \, \hat{n}' \cdot \hat{\tau} \, G(x) \right.$$

$$- \frac{k_z k_\rho^p}{k_o^2} \int d\tau' \, \breve{M}_z^p, \, \hat{\tau} \cdot \hat{R} \, G'(x)$$

$$+ \bar{\varepsilon}_p \int d\tau' \, \breve{M}_\tau^p, \left\{ (\hat{\tau} \cdot \hat{\tau}') \left[G(x) + \frac{k_\rho^p}{\bar{\varepsilon}_p k_o^2 R} G'(x) \right] \right. \tag{16}$$

$$\left. \left. + \frac{(k_\rho^p)^2}{\bar{\varepsilon}_p k_o^2} (\hat{\tau}' \cdot \hat{R})(\hat{\tau} \cdot \hat{R}) \left[G''(x) - \frac{1}{k_\rho^p R} G'(x) \right] \right\} \right] .$$

Here we have replaced the variable $\vec{M}$ by $\vec{\breve{M}}$, where

$$\vec{M}^p = -j(\varepsilon_o/\mu_o)^{\frac{1}{2}} \vec{M}^p \quad , \tag{17}$$

so that $\vec{\breve{M}}^p$ is of the same dimension as $\vec{J}^p$. $\bar{\varepsilon}_p = \varepsilon_p/\varepsilon_o$ is the relative dielectric constant of the p-th region. $k_o = \omega \sqrt{\mu_o \varepsilon_o}$ is the free space wave vector. $(\hat{n}, \hat{\tau}, \hat{z})$ and $(\hat{n}', \hat{\tau}', \hat{z}')$ denote unit vectors at the field

point (P) and the source points (P'), respectively. Also $G'(x) = \partial G(x)/\partial x$ and $G''(x) = \partial^2 G/\partial x^2$ with $x = k_p^2 R$.

If the dielectric medium of the p-th region is fictitiously extended to all space, then the tangential components of the fields at a point P_+ just outside the contour c_p are given by (See Eq.(2))

$$E_z^{p+} = E_z^{p-} + j(\mu_o/\epsilon_o)^{\frac{1}{2}} M_\tau^p \quad ,$$
$$E_\tau^{p+} = E_\tau^{p-} - j(\mu_o/\epsilon_o)^{\frac{1}{2}} \tilde{M}_z^p \quad , \tag{18}$$

$$H_z^{p+} = H_z^{p-} - j(\epsilon_o/\mu_o)^{\frac{1}{2}} J_\tau^p \quad ,$$
$$H_\tau^p = H_\tau^{p-} + j(\epsilon_o/\mu_o)^{\frac{1}{2}} J_z^p \quad . \tag{19}$$

Equations (13)-(19) for the tangential components of $\vec{E}^p$ and $\vec{H}^p$ hold for each of the dielectric regions p - 1,2, ..., N.

The following boundary conditions are now imposed for each of the N dielectric regions in the problem at hand. On the conducting surfaces

$$E_z^{p-} = 0 \quad ,$$
$$E_\tau^{p-} = 0 \quad , \tag{20}$$

and on the dielectric-dielectric interfaces

$$\left.\begin{aligned} E_z^{p+} &= 0 \ , \\ E_\tau^{p+} &= 0 \ , \end{aligned}\right\} \tag{21}$$

$$\left.\begin{aligned} E_z^{p-} - E_{z'}^{p'-} &= 0 \ , \\ E_\tau^{p-} + E_{\tau'}^{p'-} &= 0 \ , \\ H_z^{p-} - H_{z'}^{p'-} &= 0 \ , \\ H_\tau^{p-} + H_{\tau'}^{p'-} &= 0 \ , \end{aligned}\right\} \tag{22}$$

where E and H are given by equations (13)-(19). The region p' is adjacent to the p-th region in the structure shown in Fig.1. On the portion of the contour common to regions p and p', $\hat{\tau}' = -\hat{\tau}$ and $\hat{z}' = \hat{z}$. In equations (20)-(22), p = 1, 2, ..., N. Also for each p in equations (22), p' = 1, 2, ..., N_p where N_p is the number of regions adjoining the p-th region.

On substitution of equations (13)-(19) in equations (20)-(22), we obtain the set of integral equations to be satisfied by the current sources $\vec{J}^p$, $\vec{M}^p$ in all regions. $\vec{J}^p$ and $\vec{M}^p$ in the different regions are not all independent because of the boundary conditions in Equation (22). From equations (2) and (22) it is seen that

$$\vec{\tilde{M}}^p = - \vec{\tilde{M}}^{p'} \ ,$$

$$\vec{J}^p = - \vec{J}^{p'} \ ,$$

on the dielectric-dielectric interfaces.

III. MATRIX FORMULATION

The propagation characteristics are determined by solving the system of equations (13)-(22). These equations are reduced to matrix form by the method of moments [6]. The simplest approximation consists of using pulse functions for a basis and point matching for testing. For this purpose the contour c_p is divided into n^p segments and pulse functions defined as:

$$f_\beta^p(\vec{\rho}) = 1 \text{ on } \beta\text{-th segment},$$
$$= 0 \text{ on all other segments.} \tag{23}$$

The segments are not necessarily of equal length.

Let:

$$\begin{bmatrix} J_z^p \\ J_\tau^p \\ M_z^p \\ M_\tau^p \end{bmatrix} = \sum_{\beta=1}^{n_c^p} \begin{bmatrix} S_{\beta 1}^p \\ S_{\beta 2}^p \\ 0 \\ 0 \end{bmatrix} f_\beta^p + \sum_{\beta=n_c^p+1}^{n^p} \begin{bmatrix} S_{\beta 1}^p \\ S_{\beta 2}^p \\ S_{\beta 3}^p \\ S_{\beta 4}^p \end{bmatrix} f_\beta^p \,, \tag{24}$$

where

n_c^p = number of conductor segments on c_p ,

$n_d^p = n^p - n_c^p$ = number of dielectric segments on c_p .

The segment numbers have been rearranged such that $\beta = 1, 2, \ldots, n_c^p$ represent conductor segments and $\beta = n_c^p + 1, \ldots, n^p$ are dielectric segments.

On substitution of Equation (24) in Equations (13)-(22) and satisfying the resultant equations at the midpoint of each segment we obtain the following system of equations: Equations (20) and (21) become:

$$\sum_{\beta=1}^{n_c^p} P^p_{\alpha\beta} \bar{S}^p_\beta + \sum_{\beta=1}^{n_d^p} Q^p_{\alpha,\, \beta+n_c^p} \bar{\bar{S}}^p_{\beta+n_c^p} = 0 \,, \tag{25}$$

where

$$\alpha = 1, 2, \ldots, n^p \quad ,$$

$$p = 1, 2, \ldots, N \quad ,$$

and equation (22) transforms into:

$$\sum_{\beta=1}^{n_c^p} R^p_{\delta\beta} S + \sum_{\beta=1}^{n_d^p} T^p_{\delta,\, \beta+n_c^p} \bar{\bar{S}}^p_{\beta+n_c^p} + \sum_{\beta=1}^{n_c^{p'}} \bar{R}^{p'}_{\delta'\beta} \bar{S}^{p'}_\beta + \sum_{\beta=1}^{n_d^{p'}} \bar{T}^{p'}_{\delta',\beta+n_c^{p'}} = 0, \tag{26}$$

where the index δ runs over all dielectric segments common to the adjoining regions p and p'. The index δ' for the contour $c_{p'}$ refers to the same segment as the index δ for the contour c_p. A set of

equations similar to Equation (26) holds for each distinct pair (p, p') of adjacent regions. In equations (25) and (26), $\bar{S}_\beta^p$ is a 1x2 vector representing the two components of $\vec{J}_\beta^p$, the electric current source on the β-th conductor segment of contour c_p. The 1x4 vector $\bar{\bar{S}}_\beta^p$ denotes the two components of $\vec{J}^p$ and two components of $\tilde{\vec{M}}_\beta$, the current sources on the β-th dielectric segment on contour c_p. Each element $P_{\alpha\beta}^p$ is a 2x2 submatrix and each element $Q_{\alpha\beta}^p$ a 2x4 submatrix. The two rows of these submatrices correspond to the two components of $\vec{E}^p$. Similarly each element $R_{\alpha\beta}^p$ (and $\bar{R}_{\alpha\beta}^p$) is a 4x2 submatrix and each element $T_{\alpha\beta}^p$ or $\bar{T}_{\alpha\beta}^p$ a 4x4 submatrix. The four rows of these submatrices correspond to the two components of $\vec{E}^p$ and two components of $\tilde{\vec{M}}^p$ in Equation (22). The explicit forms of the matrix element of $P_{\alpha\beta}^p$, $Q_{\alpha\beta}^p$, $R_{\alpha\beta}^p$, $T_{\alpha\beta}^p$, $\bar{R}_{\alpha\beta}^p$ and $\bar{\bar{T}}_{\alpha\beta}^p$ are shown in the Appendix.

Equation (25) is a set of $2n^p$ equations in $2n_c^p + 4n_d^p$ variables for the p-th region. Equation (26) is a set of 4m equations (m being the number of dielectric segments common to regions p and p') in $2n_c^p + 4n_d^p + 2n_c^{p'} + 4n_d^{p'}$ variables of the regions p and p'. These equations for all the N regions and for all distinct pairs of adjacent regions can be manipulated in such a way that the current sources $\bar{\bar{S}}$ on the dielectric segments are expressed in terms of $\bar{S}$, the current sources on the conductor segments and then a matrix equation involving $\bar{S}$ only is obtained:

$$H\,\bar{S} = 0, \tag{27}$$

where $\bar{S}$ is a one-column vector with M components given by:

$$M = 2 \sum_{p=1}^{N} n_c^p \tag{28}$$

and H is a MXM matrix.

If the cross-section of the guiding structure is symmetrical about an axis in the transverse plane, then the problem can be reduced to modes having either even or odd symmetry with respect to this axis. In such a case, we have (for the ordering of segments as in Fig.3):

$$\begin{aligned}
\bar{S}^p_{\beta,j} &= \pm(-1)^{j+1}\ \bar{S}^p_{n_c^p + 1 - \beta,\ j} \quad , \\
\bar{\bar{S}}^p_{n_c^p + \alpha, j} &= \pm(-1)^{j+1}\ \bar{\bar{S}}_{n^p + 1 - \alpha,\ j} \quad , \\
\bar{\bar{S}}^p_{n_c^p + \alpha,\ j+2} &= \pm(-1)^{j}\ \bar{\bar{S}}^p_{n^p + 1 - \alpha,\ j+2,}
\end{aligned} \tag{29}$$

where

$$j = 1,\ 2$$

$$\beta = 1,\ 2,\ \ldots.,\ n_c^p/2 \quad ,$$

$$\alpha = 1,\ 2,\ \ldots.,\ n_d^p/2 \quad ,$$

The +(-) sign in Equation (29) applies to modes with even (odd) symmetry.

By virtue of the definitions used for $\hat{z}$ and $\hat{\tau}$, for even symmetry modes J_z and $\tilde{M}_\tau$ remain unaltered while J_τ and $\tilde{M}_z$ changes sign under reflection about the symmetry axis. The opposite is true for odd symmetry modes.

Using Equation (29) the set of equations given by Equations (25) and (26) can be reduced to the following form:

$$\sum_{\beta=1}^{n_{c/2}^p} \underset{\sim}{P}^p_{\alpha\beta} \; \bar{S}^p_\beta + \sum_{\beta=1}^{n_{d/2}^p} \underset{\sim}{Q}^p_{\alpha,\, n_{c+\beta}^p} \; \bar{\bar{S}}^p_{n_c^p+\beta} = 0 \quad , \tag{30}$$

$$\sum_{\beta=1}^{n_{c/2}^p} \underset{\sim}{R}^p_{\delta\beta} \; \bar{S}^p_\beta + \sum_{\beta=1}^{n_{d/2}^p} \underset{\sim}{T}^p_{\delta,\, n_c^p+\beta} \; \bar{\bar{S}}^p_{n_c^p+\beta}$$

$$+ \sum_{\beta=1}^{n_{c/2}^{p'}} \underset{\sim}{\bar{R}}^{p'}_{\delta'\beta} \; \bar{S}^{p'}_\beta + \sum_{\beta=1}^{n_{d/2}^{p'}} \underset{\sim}{\bar{T}}^{p'}_{\delta',\, n_c^{p'}+\beta} \; \bar{\bar{S}}^{p'}_{n_c^{p'}+\beta} = 0 \quad . \tag{31}$$

where $\alpha = 1, 2, \ldots, n^p/2$ and the index δ runs over the dielectric segments common to regions p and p' lying to the right of the symmetry axis in Fig. 3. The indices p, p' and δ' have the same meaning as in Equations (25) and (26). In equations (30) and (31), the quantities $\underset{\sim}{P}^p_{\alpha\beta}$, $\underset{\sim}{R}^p_{\alpha\beta}$ and $\underset{\sim}{\bar{R}}^p_{\alpha\beta}$ are given by the relation:

$$\left(\underset{\sim}{A}^p_{\alpha\beta}\right)_{ij} = \left(A^p_{\alpha\beta}\right)_{ij} \pm (-1)^{j+1} \left(A^p_{\alpha,\, n_c^p+\beta}\right)_{ij} \quad , \tag{32}$$

and $\underset{\sim}{Q}^p_{\sim\ell}$, $\underset{\sim}{T}^p_{\alpha\beta}$ and $\underset{\sim}{\bar{T}}^p_{\alpha\beta}$ have the form:

$$\left(\underset{\sim}{A}^p_{\alpha},\ n_c^p + \beta\right)_{ij} = \left(A^p_{\alpha,\ n_c^p + \beta}\right)_{ij} \pm (-1)^{j+1} \left(A^p_{\alpha,\ n^p+1-\beta}\right)_{ij} \quad \text{for } j = 1,2$$

$$= \left(A^p_{\alpha,\ n_c^p + \beta}\right)_{ij} \pm (-1)^{j} \left(A^p_{\alpha,\ n^p+1-\beta}\right)_{ij} \quad \text{for } j = 2,\ 3. \tag{33}$$

The (+) and (-) signs in Equation (33) apply to the even and odd symmetry modes respectively. After elimination of the variables $\bar{\bar{S}}^p_{\beta}$, an equation similar to Equation (27) is obtained where H is now of dimension (M/2) x (M/2). Because of the smaller dimension, the computation time for the calculation of the determinant of the matrix H is greatly reduced.

IV. NUMERICAL RESULTS

Since the components of the vector $\bar{S}$ in Equation (27) are all independent, a solution exists if and only if

$$\text{Det } |H(f,\ k_z)| = 0, \tag{34}$$

where $f = \omega/2\pi$ is the operating frequency and k_z is the phase constant in the direction of propagation. For a given f, the propagation constant is determined by finding k_z such that Equation (34) is satisfied. There will be several values of k_z for each f corresponding to different order modes. The cut-off frequencies for the different modes may be obtained

by searching for f such that Det $|H| = 0$ when $k_z = 0$. In general, Det $|H|$ is complex. So Equation (34) implies that

$$\text{Re}[\text{Det } H] = 0 \quad , \tag{35}$$

$$\text{Im}[\text{Det } H] = 0 \quad , \tag{36}$$

The expansion set used in Equation (24) is only an approximation to the exact current sources. Due to this approximation, the values of k_z needed to satisfy Equations (35) and (36) are, in general, slightly different. Therefore, an adequate approximate solution is obtained by requiring that:

$$|\text{Det } (H(f, k_z))| = \text{minimum.} \tag{37}$$

In actual numerical calculation a few spurious roots occur in the solution of Equation (34). The actual roots are identified by the following three criteria: (1) k_z^o that gives the deepest local minimum in $|\text{Det } H|$, (2) real and imaginary parts of Det H should change sign near k_z^o, and (3) the difference in the values of k_z satisfying Equations (35) and (36) is smallest. Also, the spurious roots shift appreciably when the number of segments in a contour is changed [1].

To illustrate the accuracy of the present method, results computed for a shielded-microstrip cross-section shown in Fig.4 are plotted in Fig.5. The calculated dispersion characteristics of the fundamental and higher order even-symmetry modes agree reasonably well with the theoretical

results in references 2 and 4. Although only even-symmetry modes are shown in Fig.5, the method is applicable to all types of modes, symmetric or otherwise.

We next show the dispersion characteristics of a channelized suspended microstrip [9]. The cross-section of the structure is shown in Fig.6. The channel located above the conducting strip helps suppress higher-order mode propagation. The structure has two additional useful features: (1) reduced dissipation loss [10], and (2) easier fabrication due to wider strip widths for 50Ω impedance level. The calculated dispersion curves are shown in Fig.7. The lower three curves represent the fundamental mode for three different values of W/H (= 1, 3, 4), the ratio of the width of the conducting strip and the height of the channel above it. The upper two curves are two higher order (even symmetry) modes for W/H = 3. The associated TEM phase constants in air and dielectric material (ϵ_r = 10.0) are shown in the figure for reference. As can be seen in Fig.7, the phase constants for the fundamental mode at lower frequencies are nearer to that in air and at high frequencies go towards the values for the dielectric medium. The cut-off frequencies for the next two even-symmetry higher order modes are 17.2 GHz and 27.4 GHz, respectively.

V. DISCUSSION

The computer-aided analyses described in this paper can determine the dispersion and higher order mode characteristics for a wide variety of transmission structures having different geometries and material

parameters. The analyses includes the effects on propagation due to an arbitrarily shaped conducting enclosure. The analyses presented here can provide design information for planar transmission media which employ composite conductor and/or dielectric materials. The analysis can be readily extended to determine other propagation characteristics such as electric and magnetic field distributions, modal currents, impedance parameters and dissipation losses.

APPENDIX

The matrices P, Q, R, $\bar{R}$, T and $\bar{T}$ in Equations (25) and (26) may be obtained in a straightforward manner by substituting Equations (13)-(19) and Equation (24) in Equations (20)-(22) as stated in the text.

The matrix elements $P^p_{\alpha\beta}$ for $\alpha \neq \beta$ are given by:

$$\left(P^p_{\alpha\beta}\right)_{11} = -\left(1 + \frac{k_z^2}{\bar{\epsilon}_p k_o^2}\right) G\left(k_\rho^p R_{\alpha\beta}\right) W_\beta \quad ,$$

$$\left(P^p_{\alpha\beta}\right)_{12} = \left(k_z k_\rho^p / \bar{\epsilon}_p k_o^2\right) G'(k_\rho^p R_{\alpha\beta}) \hat{\tau}_\beta \cdot \hat{R}_{\alpha\beta} W_\beta \quad ,$$

$$\left(P^p_{\alpha\beta}\right)_{21} = \left(k_z k_\rho^p / \bar{\epsilon}_p k_o^2\right) G'(k^p R_{\alpha\beta}) \hat{\tau}_\alpha \cdot \hat{R}_{\alpha\beta} W_\beta \quad , \tag{A1}$$

$$\left(P^p_{\alpha\beta}\right)_{22} = -\hat{\tau}_\alpha \cdot \hat{\tau}_\beta \left\{ G(k_\rho^p R_{\alpha\beta}) + \frac{k_\rho^p}{\bar{\epsilon}_p k_o^2 R_{\alpha\beta}} G'(k_\rho^p R_{\alpha\beta}) \right\} W_\beta$$

$$- \left\{ (k_\rho^p)^2 / \bar{\epsilon}_p k_o^2 \right\} (\hat{\tau}_\alpha \cdot \hat{R}_{\alpha\beta})(\hat{\tau}_\beta \cdot \hat{R}_{\alpha\beta}) \left\{ G(k_\rho^p R_{\alpha\beta}) - \frac{G''(k_\rho^p R_{\alpha\beta})}{k_\rho^p R_{\alpha\beta}} \right\} W_\beta \quad ,$$

where $R_{\alpha\beta} = |\vec{\rho}_\alpha - \vec{\rho}_\beta|$ and $\hat{R}_{\alpha\beta} = (\vec{\rho}_\alpha - \vec{\rho}_\beta)/R_{\alpha\beta}$. $\vec{\rho}_\alpha$ is the position vector of the midpoint of the m-th segment and τ_α and n_α denote, respectively the unit vectors at that point along the tangent and the normal to the contour. W_β is the width of the m-th segment. For $\alpha = \beta$

$$\left(P^p_{\alpha\alpha}\right)_{11} = (W_\alpha/2\pi)\left[\left\{\ell n \frac{k_\rho^p W_\alpha}{4} - 1 + \gamma\right\} + B\right]\left(1 + \frac{k_z^2}{\bar{\epsilon}_p k_o^2}\right),$$

$$\left(P^p_{\alpha\alpha}\right)_{22} = (W_\alpha/2\pi)\left[\left\{\ell n \frac{k_\rho W_\alpha}{4} - 1 + \gamma\right\} + B\right], \qquad \text{(A2)}$$

$$\left(P^p_{\alpha\alpha}\right)_{12} = \left(P^p_{\alpha\alpha}\right)_{21} = 0,$$

where γ is the Euler Constant and $B = \frac{i\pi}{2}$ if $(\bar{\epsilon}_p k_o^2 + k_z^2) \gtrless 0$ while $B = 0$ if $(\bar{\epsilon}_p k_o^2 + k_z^2) < 0$.

The matrix elements $Q^p_{\alpha\beta}$ are given by:

$$\left(Q^p_{\alpha\beta}\right)_{ij} = \left(P^p_{\alpha\beta}\right)_{ij} \quad \text{for} \quad \begin{matrix} i = 1, 2 \\ j = 1, 2 \end{matrix},$$

and

$$\left(Q^p_{\alpha\beta}\right)_{14} = (k_\rho^p/k_o)\, G'(k_\rho^p R_{\alpha\beta})\, \hat{n}_\beta \cdot \hat{R}_{\alpha\beta}\, W_\beta,$$

$$\left(Q^p_{\alpha\beta}\right)_{13} = 0, \qquad \text{(A3)}$$

$$\left(Q^p_{\alpha\beta}\right)_{24} = (k_z/k_o)\, \hat{n}_\beta \cdot \hat{\tau}_\alpha\, G(k_\rho^p R_{\alpha\beta})\, W_\beta,$$

$$\left(Q^p_{\alpha\beta}\right)_{23} = -(k_\rho^p/k_o)\, \hat{n}_\alpha \cdot \hat{R}_{\alpha\beta}\, G'(k_\rho^p R_{\alpha\beta})\, W_\beta,$$

for $\alpha \neq \beta$, and

$$\left.\begin{aligned} \left(Q^{p}_{\alpha\alpha}\right)_{14} &= -\left(Q^{p}_{\alpha\alpha}\right)_{23} = 1/2k_{o} \quad , \\ \left(Q^{p}_{\alpha\alpha}\right)_{13} &= \left(Q^{p}_{\alpha\alpha}\right)_{24} = 0 \quad , \end{aligned}\right\} \tag{A4}$$

for $\alpha = \beta$.

The expressions for $R^{p}_{\alpha\beta}$ are:

$$\left(R^{p}_{\alpha\beta}\right)_{ij} = \left(Q^{p}_{\alpha\beta}\right)_{ij} \quad \text{for} \begin{cases} i = 1, 2 \\ j = 1, 2 \end{cases} \tag{A5}$$

and

$$\left.\begin{aligned} \left(R^{p}_{\alpha\beta}\right)_{31} &= -\left(Q^{p}_{\alpha\beta}\right)_{13} \quad , \\ \left(R^{p}_{\alpha\beta}\right)_{32} &= -\left(Q^{p}_{\alpha\beta}\right)_{14} \quad , \\ \left(R^{p}_{\alpha\beta}\right)_{41} &= -\left(Q^{p}_{\alpha\beta}\right)_{23} \quad , \\ \left(R^{p}_{\alpha\beta}\right)_{42} &= -\left(Q^{p}_{\alpha\beta}\right)_{24} \quad , \end{aligned}\right\} \tag{A6}$$

while that for $T^{p}_{\alpha\beta}$ are:

$$\left.\begin{aligned} \left(T^{p}_{\alpha\beta}\right)_{ij} &= \left(R^{p}_{\alpha\beta}\right)_{ij} \quad , \; i = 1, 2, 3, 4 \text{ and } j = 1, 2 \\ \left(T^{p}_{\alpha\beta}\right)_{ij} &= \left(Q^{p}_{\alpha\beta}\right)_{ij} \quad , \; i = 1, 2 \text{ and } j = 3, 4 \end{aligned}\right\} \tag{A7}$$

and

$$\left.\begin{aligned}
\left(T^{p}_{\alpha\beta}\right)_{34} &= -\bar{\epsilon}_{p}\left(Q^{p}_{\alpha\beta}\right)_{12} \quad , \\
\left(T^{p}_{\alpha\beta}\right)_{33} &= -\bar{\epsilon}_{p}\left(Q^{p}_{\alpha\beta}\right)_{11} \quad , \\
\left(T^{p}_{\alpha\beta}\right)_{44} &= -\bar{\epsilon}_{p}\left(Q^{p}_{\alpha\beta}\right)_{22} \quad , \\
\left(T^{p}_{\alpha\beta}\right)_{43} &= -\bar{\epsilon}_{p}\left(Q^{p}_{\alpha\beta}\right)_{21} \quad .
\end{aligned}\right\} \tag{A8}$$

Finally,

$$\left(\bar{R}^{p}_{\alpha\beta}\right)_{ij} = (-1)^{i}\left(R^{p}_{\alpha\beta}\right)_{ij} \quad , \tag{A9}$$

and

$$\left(\bar{T}^{p}_{\alpha\beta}\right)_{ij} = (-1)^{i}\left(T^{p}_{\alpha\beta}\right)_{ij} \quad , \tag{A10}$$

to account for the alternate "+" and "-" signs on the left-hand side of the four equations in Equation (22).

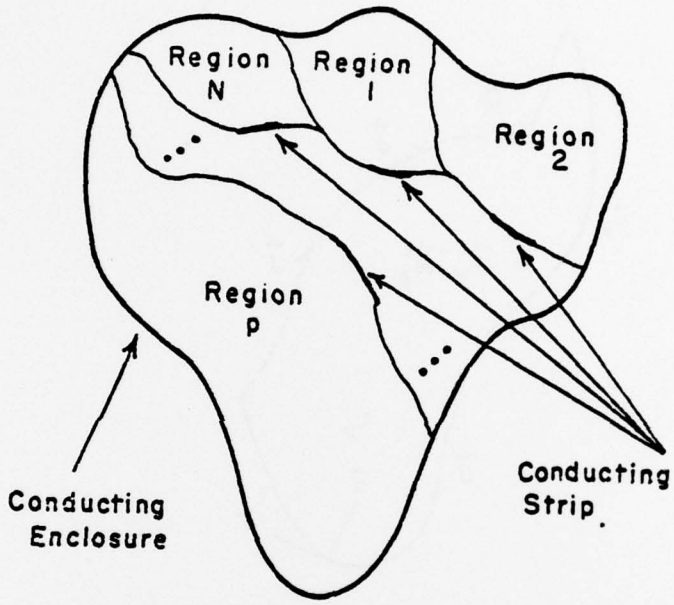

Fig. 1. Generic cross-section of mixed conductors and dielectrics in conducting enclosure

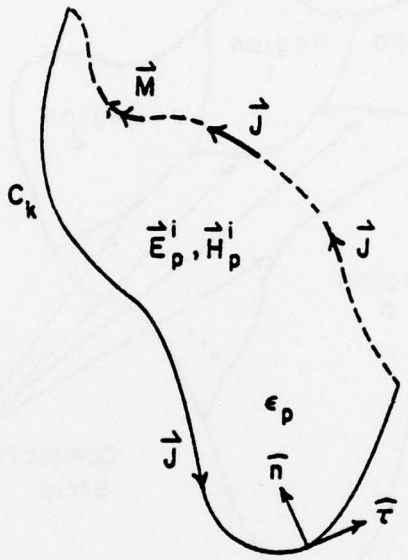

Fig. 2. Conceptual treatment of currents and fields for the p-th region. τ, $\hat{n}$ and $\hat{z}$ are unit vectors along three orthogonal coordinates axes used in the text. $\hat{z}$ is normal to the plane of the paper pointing up.

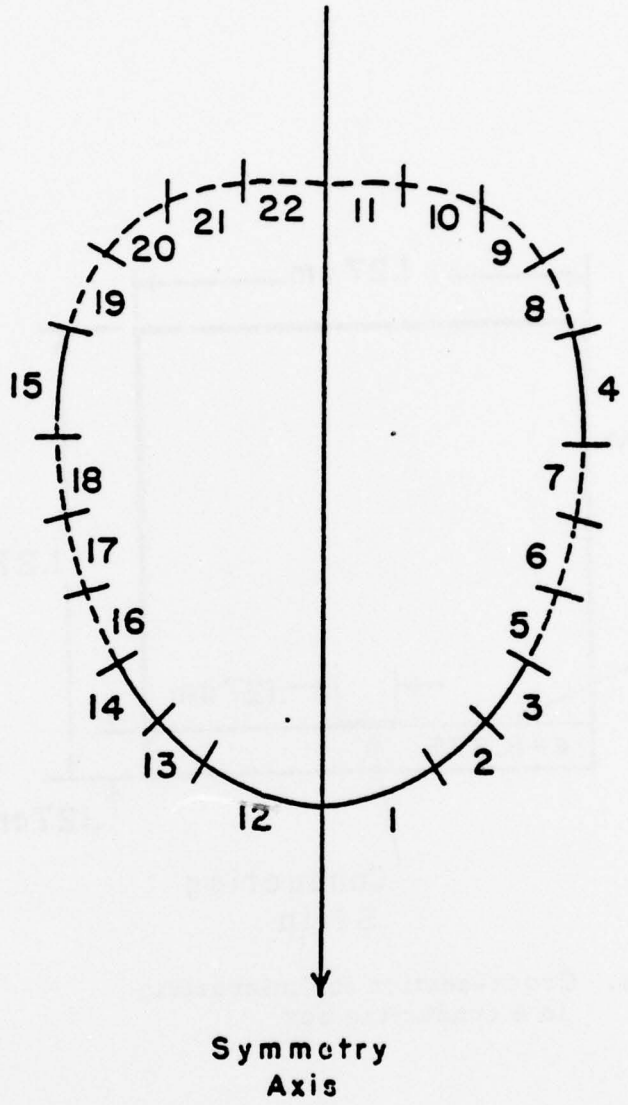

Fig. 3. Symmetric waveguide cross-section showing the ordering of the segments for a case with $n^P = 22$, $n_c^P = 8$, and $n_d^P = 14$

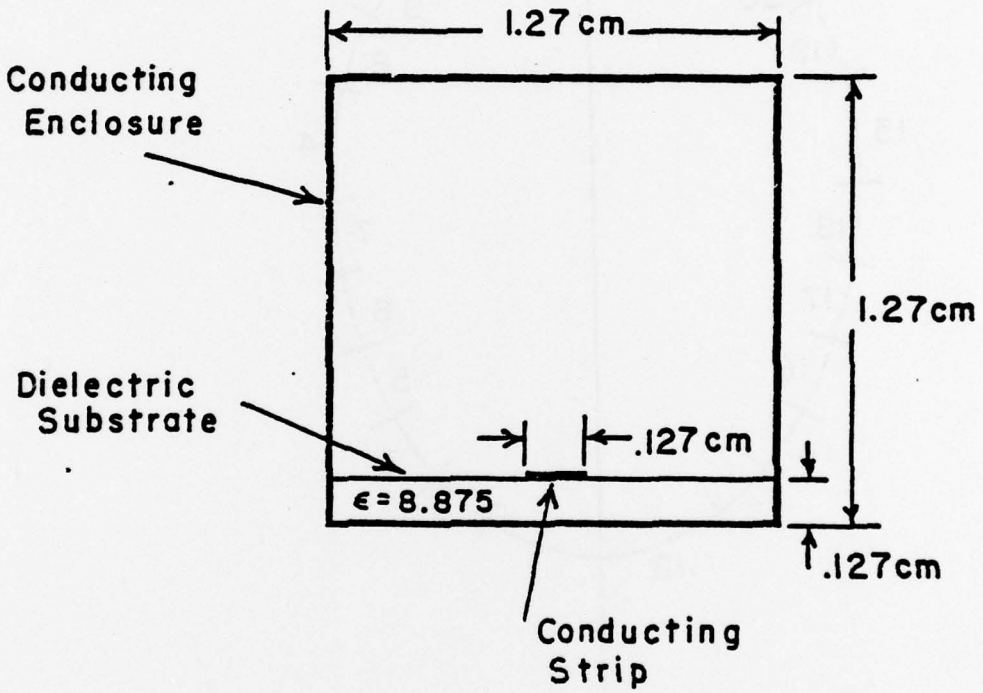

Fig. 4. Cross-section for microstrip in a conducting box

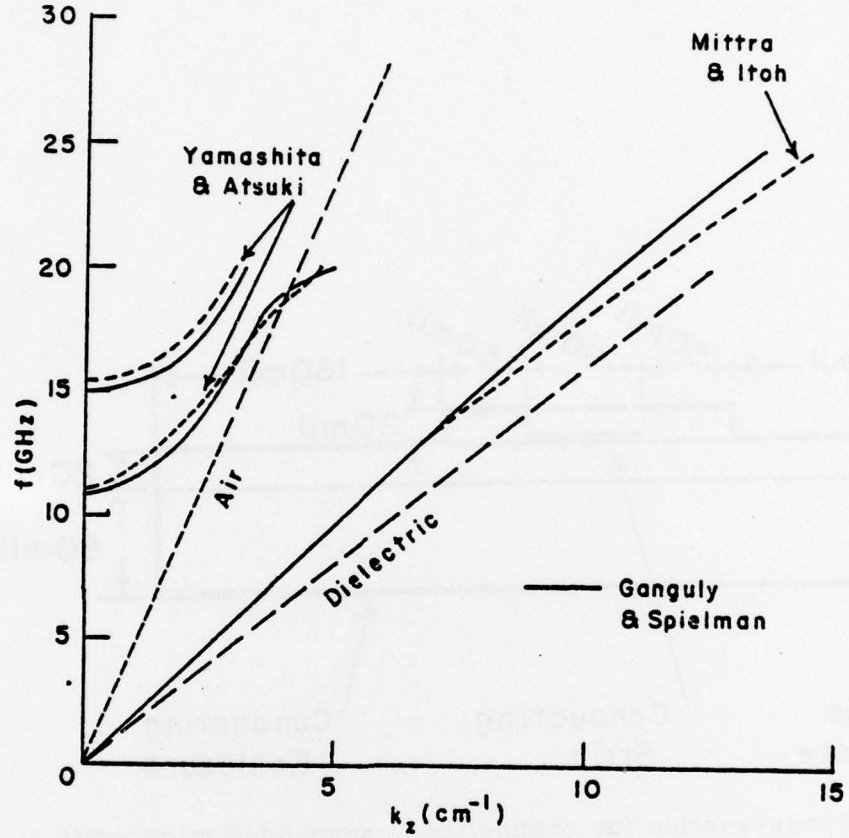

Fig. 5. Dispersion characteristics for microstrip in a conducting box

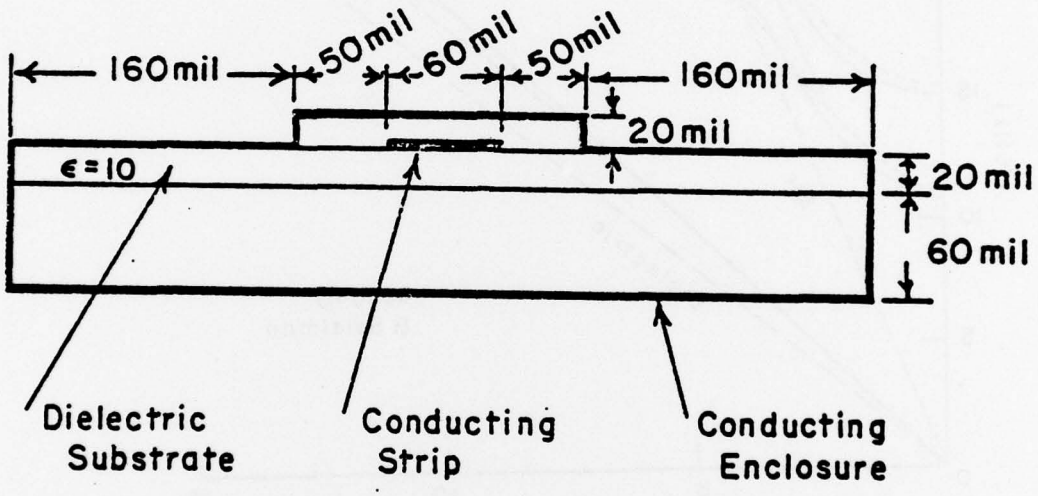

Fig. 6. Cross-section for channelized, suspended microstrip

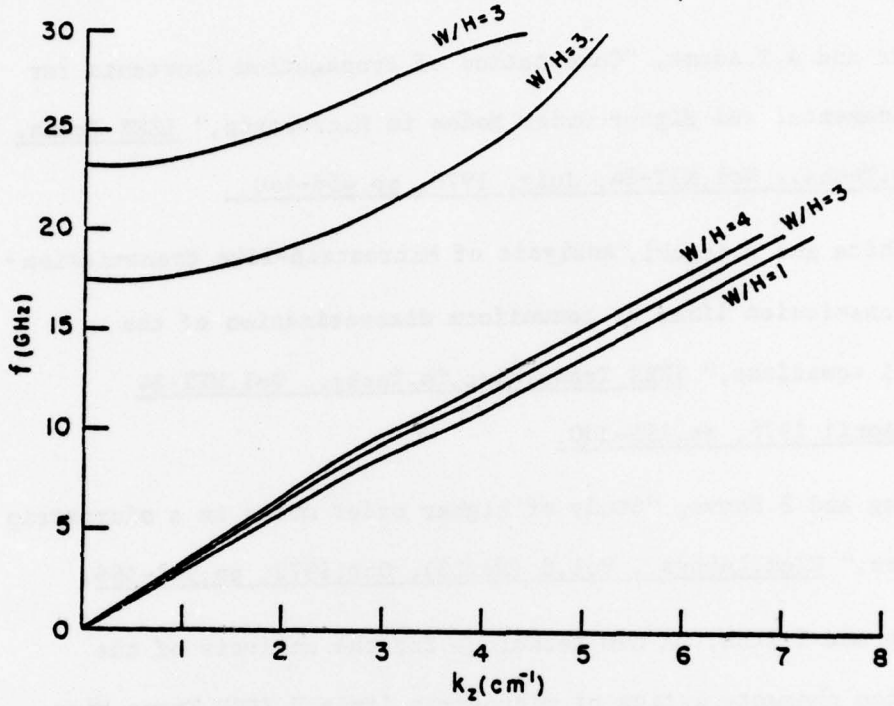

Fig. 7. Dispersion characteristics for channelized suspended microstrip. W = width of the conducting strip and H = height of the channel above it.

REFERENCES

1. A.Farrar and A.T.Adams, "Computation of Propagation Constants for the Fundamental and Higher Order Modes in Microstrip," IEEE Trans. Micr.Th.Techs., Vol.MTT-24, July, 1976, pp.456-460.

2. E.Yamashita and K.Atsuki,"Analysis of Microstrip-like transmission-like transmission lines by nonuniform discretization of the integral equations," IEEE Trans.Micr.Th.Techs., Vol.MTT-24 (No.4),April 1976, pp.195-200.

3. G.Essayag and B.Sauve, "Study of higher order modes in a microstrip structure," Elec.Lettrs., Vol.8 (No.23), Oct.1972, pp.564-566.

4. R.Mittra and T.Itoh, "A new technique for the analysis of the dispersion characteristics of microstrip lines," IEEE Trans.Micr. Th.Techs., Vol.MTT-19 (No.1) Jan. 1971, pp.47-55.

5. R.F.Harrington, Time Harmonic Electromagnetic Fields, McGraw-Hill Book Company, 1961, pp.106-110.

6. R.F.Harrington, Field computation by moment methods, McMillan Co., 1968, pp.11.

7. Ibid, Chapter 1, pp.9-11.

8. Ibid, Chapter 1, pp.14-15.

9. A.K.Ganguly and B.E.Spielman, "Dispersion in Arbitrarily-Configured Dielectric Loaded Transmission Structures,"1977 IEEE/MTT-S International Microwave Symposium Digest, San Diego, CA (To be published,1977); and IEEE Micr.Th.Techs.Trans., (To be published)

10. B.E.Spielman, "Computer-aided analysis of dissipation losses in isolated and coupled transmission lines for microwave and millimeter wave integrated-circuit applications," NRL Report #8009, Naval Research Laboratory, Washington, DC, July 1976, p.28.